

Visible Light Assisted Degradation of Eosin Yellow using Heteroatom Functionalized TiO₂ Nanomaterial.

Desta Shumuye Meshesha^a, Siva Rao Tirukkovalluri^{a*}, Matangi Ravi Chandra^a, Sreedhar Bojja^b

a. Department of Inorganic and Analytical Chemistry, Andhra University, Visakhapatnam 530003, India.

b. Department of Inorganic & Physical Chemistry Division, Indian Institute of Chemical Technology, Hyderabad 500007, India.

Corresponding author. Tel.: +91 7702110459.

E-mail address: sivaraotvalluri.l6@gmail.com (T. Siva Rao)

ABSTRACT

10 ppm EY dye were successfully photodegraded using visible light active 0.75wt% Ba & 0.25wt% Zr co-doped TiO₂ nanomaterial that were synthesized by Sol-gel method as nanomaterials under irradiation for 20 minutes and characterized by various advanced instrumental techniques. The X-ray Diffraction Spectroscopic showed that the prepared nanomaterial were in the anatase phase with 2θ at 25.3°. UV-visible Diffuse Reflectance Spectra analysis explained that the dopants found in the TiO₂, imparts a significance absorption shift towards visible region and their existence were confirmed by X-ray Photoelectron Spectral data.

Quantitatively the formation of hydroxyl radical by the nanomaterial in aqueous solution under visible light irradiation was investigated by the photoluminescent technique. Finally the effects of different parameters in the photocatalytic degradation of EY were established in aqueous solution.

Key words: - Eosin yellow, EY, hydroxyl ion, photoluminescent.

I. Introduction

Industrial uprising and the day to day human activities have influenced on the flow, Storage and the quality of available fresh water. Dyes are used in food; textiles, beverage industries and printing processes and throughout the processes huge volumes of water consume by textile industries and generate huge quantities of colored dye effluents [1-3]. Natural streams and rivers are extremely poisoned when untreated colored effluents discharged to the water bodies that causes chemical as well as biochemical changes and consumes dissolved oxygen and destroy aquatic life [4-6]. Eosin Yellow is a heterocyclic dye containing bromine atoms, specifically used in the fields of dyeing, printing, leather, printing ink and fluorescent pigment etc, because of its vivid color. Coagulation/ flocculation, membrane separation (ultra filtration, reverse osmosis) or absorption at activated carbon, are mostly conventional techniques, based on phase transfer mechanism of the pollutant.

Colored dyes owing to their complex chemical structures, they are resistant to biodegradation and are hardly removed from effluents using wastewater conventional treatments.

But advanced oxidation processes (AOPs), using semiconductor/heterogeneous photocatalysis appear as the most emerging destructive technology with the possibility of using sunlight as the source of irradiation to initiate the demolition of organic pollutants [7]. Titanium dioxide (TiO₂) is the most widely used photocatalyst which is a newly growing technology and highly promising, cheap, stable, nontoxic, and efficient free from secondary pollutants for serving of environmental purification and best as well as appropriate photocatalyst [8, 9]. It is known that out of the incoming solar energy on the Earth's surface only 4% can be utilized by titania because of the relatively high intrinsic band gap of anatase TiO₂ (3.2 eV), The main drawback associated with its use is, the activated charge carriers before reaching the surface to interact with adsorbed

molecules will undertake recombination leading to low photoactivity of TiO₂ within a nanosecond after their generation. Avoiding of this limitation, and to get better light absorption feature characteristics and to extend the photocatalytic carrier life time, to extend visible light response of TiO₂, doping and co-doping of metals, non metals or metal & nonmetal found to be most suitable [10-13]. Nitrogen-doped TiO₂ was considered to be a promising by reducing of the band gap making it visible light active photocatalyst and metal dopants facilitate the charge separation of e⁻/h and thus decrease their rate of recombination [14].

Studies on Synthesis of a series of Zr & S co-doped TiO₂ (Zr-TiO₂-S) prepared by a modified Sol-gel method were also developed for degradation of pollutants [15]. Studied on the feasibility of a novel adsorbent composite photocatalyst, poly (pyrrole-co-aniline)-coated TiO₂/nanocellulose composite (P (Py-co-An)-TiO₂/NCC), utilized to remove EY from aqueous solutions [16]. Therefore to have powders of homogenous concentrations synthesized at low temperatures with high purity under stoichiometry control Sol-gel method is helpful [17]. In view of the significance of visible light responsive photocatalyst, it is much honored to use a photocatalyst with appropriate particle size, phase, and other surface properties. Hence sol-gel method has been followed for the preparation of barium and zirconium co-doped TiO₂ (Ba & Zr co-doped TiO₂) nanomaterial.

II. Synthesis of nanomaterial photocatalyst.

A series of TiO₂ samples were prepared by co-doping with barium and zirconium in the range of 0.25 –1.25 wt% and undoped TiO₂ by sol-gel method. For undoped TiO₂ preparation, ethanol is taken as solvent and added to titanium tetrabutoxide (titanium precursor) for having hydrolysis and condensation reactions in presence of nitric acid with continuous string followed by addition of ethanol and water drop wise after 30 minute. In case of co-doped catalyst preparation, calculated quantities of barium nitrate and zirconyl nitrate, (precursors of Ba and Zr,) respectively were initially dissolved in water along with ethanol and the resultant solution was added drop by drop from the burette to the ethanol solution of Ti (OBu)₄

under vigorous stirring. After addition is over, the colloidal suspension was allowed to stir for 60 min and aged for 48 hrs in the drake. The formed gel was dried in an oven at 100°C. Afterward, it was well pulverized before and after calcinations at 450°C for 2 hrs in muffle furnace then cooled the homogenous nano powder form.

III. Characterization of Photocatalyst.

XRD spectra were recorded for 2θ from 20° to 80° with model Ultima IV, RIGAKU diffractometer using monochromatized CuKα radiation (λ = 1.541 Å) with a Germanium solid state detector. The crystallite size of the nanoparticles was calculated from sheerer equation, XPS studies were done using PHI quantum ESCA microprobe system model, using AlKα radiation of 250W X-ray tube as a radiation source with energy of 1486.6 eV, 16mA ×12.5 kV under working pressure lower than 1 ×10⁻⁸ Nm⁻². The fitting of the XPS curves was analyzed with multi pack 6.0A software. UV-visible absorption spectra of the samples were obtained by using Shimadzu 3600, UVvisible NIR spectrophotometer using BaSO₄ as reference scatter. Photoluminescent spectral analysis was done using Horiba Jobin Fluoro Max-4 instrument with a PMT voltage of 150V and slit set both at 2.5 nm.

IV. Photocatalytic activity of the nanomaterial catalyst.

For the establishment of adsorption desorption equilibrium on the nanomaterial catalyst surface, a dye solution with catalyst was stirred in dark for 20 min. The reaction mixture was exposing to visible light source of 400W high pressure mercury vapor lamp (Osram, India) by placing it 20 cm away from light source. Aliquots of samples were withdrawn at a certain regular time intervals, through 0.45 μm Millipore syringe filter. The filtrate was analyzed on spectrophotometer at a wavelength of 517 nm for (%) percentage degradation studies of EY. To have a comprehensive idea of the reaction environment it is necessary to maintain the same for all the activity tests. Percentage degradation of the dye was calculated from the following equation:

$$\% \text{ Degradation} = [(A_0 - A_t) / A_0] \times 100$$

Where A_0 is initial absorbance of dye solution before degradation and A_t is absorbance of dye solution at time t .

V. Results and Discussions

5.1 X-ray Diffraction Spectroscopic (XRD)

XRD patterns of Ba and Zr co-doped TiO₂ nanoamaterial samples and undoped titania sample were prepared by sol-gel method and calcined at 450°C shows in Fig.5.1. All the samples are in anatase phase (JCPDS No.: 21-1272) with corresponding (1 0 1) plane at $2\theta = 25.3^\circ$ followed by 2θ of 37.7° , 47.9° , 54.1° , 55° and represents the planes (004), (200), (105), (211) anatase TiO₂ respectively. Moreover, it was observed that, when the dopant Ba²⁺ concentration increases from 0.25wt% to 0.5wt%, it was not observed any respective peaks of barium oxide. After increasing the concentration of Ba²⁺ as 0.75wt% and 1.0wt%, it was observed which corresponds to the formation of BaCO₃ [10]. On the other side, there is also no detectable dopant Zr⁴⁺ related peaks were observed. Hence, the Zr⁴⁺ may be occupied substitutional sites of the TiO₂ crystal structure and it is more electro positive than TiO₂ which favors the formation of less dense anatase phase [18]

5.2. Ultraviolet-Visible Diffuse Reflectance Spectroscopic studies.

The UV-visible DRS spectrum of prepared samples was shown in Fig.5.2. From the UV-visible DRS studies the characteristic band for the prepared samples was in the range of 380 to 500 nm, and the band gap energy (eV) for the selected samples calculated using $E=1240/\lambda$ (where as λ is wavelength). The band gap of synthesized undoped TiO₂ was found to be 3.17 eV which is comparable with the literature value. The co-doped samples showed band gap ranging from 2.63 to 3.02 eV. Hence lowering of the band gap, imparts the absorbance shifted from ultraviolet to visible region. Thus Red shift indicates more photogenerated e⁻/h⁺ pairs that could be excited by photons with less energy, lead to better photocatalytic efficiency in the visible region. Thus, the results confirmed that all the synthesized co-doped samples had reduced band gap and are active in visible region.

5.3 Transmission electron microscope (TEM) analysis

Tem image of 0.75 wt. % Ba and 0.25 wt. % Zr co-doped TiO₂ was represented in Fig.5. 3 and average particle size was found to be 20.63nm. It is in good agreement with the results of crystallite size calculated by using the Scherer equation and the full width at half maximum of the (101) peak in the XRD patterns of the material. Ba & Zr co-doping into TiO₂ brings in decrease of the crystallite size of TiO₂ which leads to increase of surface area of the catalyst, which is favorable precondition for higher photocatalytic activity.

Based on XRD data and trail photocatalytic activity studies, further characterization has been made for Ba & Zr co-doped TiO₂ nanoamaterial which showed best in trail photocatalytic degradation activity studies.

5.4. X-Ray Photoelectron Spectroscopic (XPS) Analysis.

XPS analysis of Ba & Zr co-doped nanoamaterial was carried out to authenticate the presence of Ba and Zr and investigate their chemical state. The high resolution XPS spectra of Ba & Zr co-doped nanoamaterial with elemental analysis of Ti, O, Ba, and Zr were represented in Figure 5.4. The co-doped Showed two peaks of Zr_{3d_{5/2}} and Zr _{3d_{3/2}} are absorbed with a binding energy of 178.332 and 181.063 eV respectively, this can be attributed to Zr⁴⁺. From the above XPS results a 3d peaks at 781.171 eV and 795.874 eV corresponding to _{3d_{5/2}} and _{3d_{3/2}} respectively are assigned as Ba²⁺ and does not absorbed into the TiO₂ being it is high atomic radii than Ti. The XPS spectra of undoped TiO₂ show spin orbit doublet peaks of Ti 2p_{3/2} and 2p_{1/2} located at 459.0 and 464.7 eV which indicating the presence of Ti⁴⁺ in the synthesized nanopowders [19,20]. Thus the presence of Zirconium has certain influence on Ti⁴⁺ pulling the electrons in Ti–O–Ti bond, a bit away from Ti atom, thus causing a little rise in Ti 2p_{3/2} binding energy. Thus XPS data has confirmed that there is a substitutional doping of Zr in TiO₂ network.

5.5. Photoluminescent Spectral Studies

The decisive reactive species during photocatalytic reaction is formation of hydroxyl radical which is a responsible for oxidative decomposition of pollutants. To investigate the production of $\cdot\text{OH}$, one of the methods is photoluminescence technique. Coumarone is used as a fluorescent probe, which on reaction with $\cdot\text{OH}$ results in the formation of 7-hydroxy coumarone [21]. In this technique, 0.1g of catalyst is dispersed in 10 ppm of coumarone 100 mL aqueous solution in acidic conditions and exposed to visible light radiation. For every 30 min 5 mL of the reaction solution was taken and filtered and photoluminescent intensity was measured from 350 to 600 nm. The photoluminescent spectra of the generated 7-hydroxy coumarone with maximum absorption at 450 nm showed in Fig. 5.5. Increasing of photoluminescent intensity was observed linearly with increasing irradiation time for first excitations. However, no maximum absorption is observed for the sample in absence of irradiation (0 min). Hence this indicates that, the produced $\cdot\text{OH}$ at the catalyst surface was proportional to the irradiation time. The results further confirmed that, the selected synthesized sample of Ba & Zr co-doped TiO_2 nanomaterial showed better rate of formation of $\cdot\text{OH}$.

VI. Photocatalytic Degradation of EY.

Photocatalytic degradation of EY was performed using the procedure given in Section 1.1. A blank test of the dye without photocatalyst is also performed and there was no change of dye concentration observed. The photocatalytic performance depends on certain parameters, these parameters are mainly focused on dopant concentration, catalyst dosage, pH of solution and initial dye concentration, and hence optimization of these parameters must be necessary to be cost effective.

6.1. Effect of Dopant Concentration.

Photocatalytic degradation studies of synthesized different nanomaterial catalyst of various dopant concentrations on EY are presented in Fig. 6.1. All the co-doped samples showed higher photocatalytic activity than that undoped titania, under visible light irradiation. So, it is a

manifest to say that co-doping enhances the photocatalytic performance of TiO_2 . Among all the co-doped nanomaterials 0.75wt% Ba & 0.25wt% Zr co-doped TiO_2 showed better percentage of photocatalytic degradation.

Regarding to the above analysis, the optimal Ba and Zr content is so small hence with over dosage of dopant content in TiO_2 , the number of e^-/h^+ recombination centers will increase which accompanied with low photocatalytic activity.

6.2. Effect of pH solution

Fig.6.2. Represents the percentage degradation of EY as function of time at different pH values. A nanomaterial exhibiting best photocatalytic performance of 0.75wt% Ba & 0.25wt% Zr co-doped TiO_2 was selected and experiments were conducted for finding the optimum pH at constant dye concentration of 10 ppm and catalyst dose of 0.1g. As we have observed from the figure photo degradation of this anionic dye was faster at pH 2.

During photocatalytic degradation, electrostatic interactions among a semiconductor surface, substrate, and charged radicals strongly depend on the pH of the solution. At lower pH environment, positive charge on TiO_2 surface increases which enhances the adsorption of dye molecules on the surface of catalyst, in addition to minimizes the e^-/h^+ recombination. But at higher pH TiO_2 surface develops negative charges that occurs repulsion with a dye molecule that imparts in low adsorption of molecule leading to low degradation efficiency.

6.3. Effect of Catalyst Dosage

An optimum catalyst concentration must be decided in order to avoid wastage of catalysts and ensure the total absorption of photons. Photocatalytic degradation was carried out upon using varying dosage from 0.25-0.3g of the selected co-doped TiO_2 nanomaterial at pH 2 is represented in fig. 6.3 Linear increase rate of degradation observed with increase in amount of catalyst up to 0.2g.

The number of photons absorbed by the catalyst is high as of the catalyst dosage is

increase, which in turn increases the generation of electrons and holes and thus increases the number of hydroxyl radicals. Hence it absorbs also more dye molecules. However, beyond 0.2g of catalyst dosage, photocatalytic activity decreased due to the turbidity, restriction of light penetration that acts as blanket. Since high catalyst dosage significantly affects the degradation

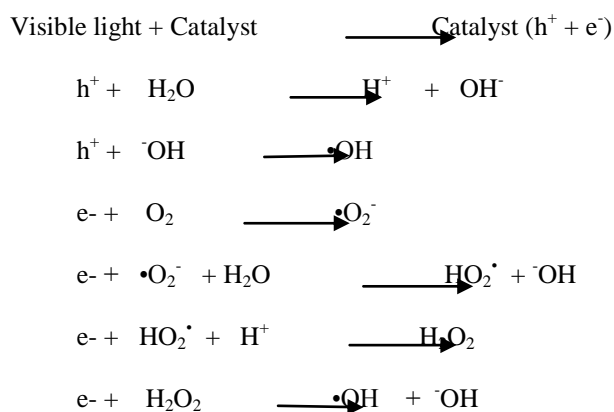
6.4. Effect of Initial Concentration of Dye.

To decide the optimum initial dye concentration at a fixed catalyst dosage and pH,

experiments were conducted with different dye concentrations of 5, 10, 15, and 20 ppm and results are represented in Fig. 6.4.

The optimum initial concentration of dye was found to be 10 ppm and further increase in dye concentration decreased the rate of degradation. For this reason as the dye concentration increases, the corresponding ratio of reactive species ($\cdot\text{OH}$) may not be formed at the fixed catalyst dosage. Restriction of surface active sites for the catalytic reaction may also control the degradation of EY.

6.5. Mechanism in formation of $\cdot\text{OH}$ (hydroxyl radical).



VII. Conclusion

Barium and zirconium were effectively co-doped TiO_2 and its photocatalytic activity was studied for the degradation of EY under visible light. All the synthesized samples were in anatase phase and band-gap has been reduced. Co-doping improved the trapping of electrons inhibiting e^-/h^+ recombination during photocatalytic process. Among all the synthesized catalysts 0.75wt.% Ba and 0.25wt.% Zr co-doped TiO_2 nanomaterial exhibited excellent photocatalytic activity under visible light due to large shift in band gap, high crystalline anatase phase, and effective separation of electrons and holes. 100% degradation of EY with initial concentration of 10 ppm was achieved in 20 min at pH 2 with catalyst dosage of 0.1g. The experimental results revealed that eosin yellow can be effectively degraded by Ba & Zr co-doped TiO_2 nanomaterial.

VIII. Acknowledgments

Thankful to **University of Gondar (UOG) Ethiopia, Government of the Federal Democratic Republic of Ethiopia** for their giving me a chance to pursue PhD, My Research Guide **Prof.T.siva Rao** for his unlimited help and encouraging me. Advanced Analytical Laboratory, DST-PURSE Programme, and Andhra University for their support in carrying out in this research work regarding SEM-EDX, FT-IR, XRD analysis. **Prof. Sreedhar Boja** (IICT- Hydra bad (India) for their unlimited support in carrying out in this research work regarding characterization of nanomaterials using advanced instruments such as TEM, XPS, UV-visible DRS ,BET and XRD.

REFERANCE

- [1] R. Ahmed, R. Kumar, Adsorptive removal of Congo red dye from aqueous solution using bael shell carbon, *Appl. Surf. Sci.* 257, 2010, 1628-1633.
- [2] N.S. Arul, D. Mangalaraj, J.I. Han, Photo electrochemical degradation of eosin yellowish dye on exfoliated graphite-ZnO nanocomposite electrode. *J. Mater. Sci. Mater. Electron.* 26, 2015, 1441-1448.
- [3] B.R. Babu, A.K. Parande, S. Raghu, K. Prem, T. Cotton. Textile Processing: Waste Generation and Effluent Treatment. *J. Cotton Sci.* 11, 2007, 141-153.
- [4] O. Abdelwabb. N.K. Amin, Adsorption of phenol from aqueous solutions by *Luffa cylindrica* fibers: Kinetics, isotherm and thermodynamic studies. *The Egyptian J. of Aquatic Research.* 39, 2013, 215-223.
- [5] H. Hameed, J. Hazard. Spent tea leaves: a new non-conventional and low-cost adsorbent for removal of basic dye from aqueous solutions. *Mater.* 161, 2009, 753-759
- [6] N. Emmanuel, G. Kumar, Environ. Chem. Photo detoxification of solubilized vat dye effluent using different pH ranges. *Lett.* 7, 2009, 375-379.
- [7] J. Rathousky, V. Kalousek, M. Kolar, J. Jirkovsky, Mesoporous films of TiO₂ as efficient photocatalysts for the purification of water. *Photochem. Photobiol. Sci.* 10, 2011, 419-424.
- [8] L.M. AL-Harbi, E.H. El-Mossalamy. Effect of RE Dopant (Ce & Tb) on PL and Crystallites size of Lanthanum Phosphor (LaPO₄). *Appl. Sci.* 5, 2011, 130-135.
- [9] N. Banerjee, The design, fabrication, and photocatalytic activity of nanostructured semiconductors: focus on TiO₂-based nanostructures. *Nanotechnol. Sci. Appl.* 4, 2011, 35-65
- [10] R. Guido, M. Jacques, G. Michael, S. Nick, K.S. Devendra, Charge carrier trapping and recombination dynamics in small semiconductor particles, *J. of the American Chemical Society*, 107 (26), 1985, 8054-8059
- [11] Y. Hua, L. Xin-Jun, Z. Shao-Jian, X. Wei. Photocatalytic activity of TiO₂ thin film non-uniformly doped by Ni. *Materials Chemistry and Physics*, 97, 2006, 59-63
- [12] N. Narayanan, Z.Y. Binitha, R. Ramakrishnan, Influence of synthesis methods on zirconium doped titania photocatalysts. *Cent. Eur. J. of Chem.* 8(1), 2010, 182-187
- [13] E.W. McFarland, H. Metiu, W. Eric. M. Farland, and M. Horia, *Catalysis by doped oxides.* *Chem Rev*, 113, 2013, 4391-4427.
- [14] A. Fujishima, X. Zhang, D.A. Tryk, TiO₂ photocatalysis and related surface phenomena. *Surf Sci .Rep*, 63, 2008, 515-582.
- [15] R. Asahi, T. Morikawa, T. Ohwaki, K. Aoki. Y. Taga, Visible-light photocatalysis in nitrogen-doped titanium oxides. *Science*, 293, 2001, 269-271.
- [16] R. Khan, S. Kim, W. Kim, T.J. Lee, Preparation and application of visible-light-responsive Ni-doped and SnO₂-coupled TiO₂ nanocomposite photocatalysts. *J. Hazard Mater.* 163(2-3), 2009, 1179-84
- [17] T.S. Anirudhan, and R.S. Rejeena, Photocatalytic Degradation of Eosin Yellow Using Poly(pyrrole-co-aniline)-Coated TiO₂/Nanocellulose Composite under Solar Light Irradiation Hindawi Publishing Corporation. *J. of Materials Volume* 2015, Article ID 636409, 11
- [18] P. Jongee, K. Derya, O. Abdullah, Sol-gel synthesis and photocatalytic activity of B and Zr co-doped TiO₂. *J. of Physics*

and *Chemistry of Solids* , 74, 2013, 1026–1031

[19] N. Venkatachalam, M. Palanichamy, V. Murugesan, Sol-gel preparation and characterization of alkaline Earth metal doped nano TiO₂ efficient photocatalytic degradation of 4-chlorophenol, *Journal of molecular catalysis A: chemical* 273, 2007, 177-185

[20] M. Zhang, X. Yu, D. Lu, and J. Yang, Facile synthesis and enhanced visible light photocatalytic activity of N and Zr co-doped TiO₂ nanostructures from nanotubular titanic acid precursor, *Nanoscale Research Letters*, 8, 2013, 1-8.

[21] H. Czili, and A. Horvath, Applicability of coumarin for detecting and measuring hydroxyl radicals generated by photoexcitation of TiO₂ nanoparticles. *Applied Catalysis B: Environmental*, 81, no. 3-4, 2008, 295–302,

Table 1. Shows crystallite size, Band gap and BET surface area of the prepared co-doped and Undoped nanomaterials.

Catalyst	Crystallite size	Band gap
0.75wt% Ba & 0.25wt% Zr-TiO ₂	20.15 nm	2.689 eV
Undoped	36.55 nm	3.17 eV

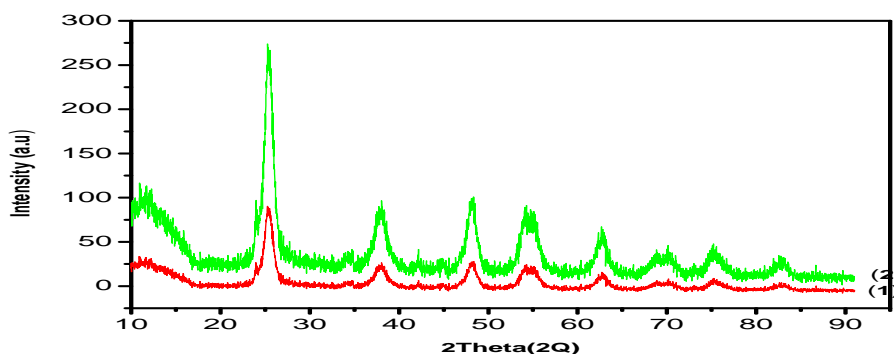


Fig. 5.1. XRD pattern of the synthesized undoped and 0.75wt% of Ba²⁺ & 0.25 wt% Zr⁴⁺ co-doped TiO₂

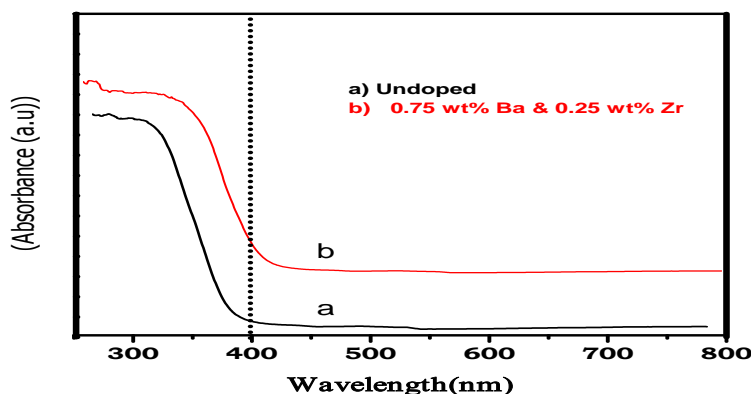


Fig.5.2. The UV-vis-DRS spectra of, undoped and co-doped TiO₂ 0.75 wt.% of Ba²⁺ and 0.25wt% Zr⁴⁺.

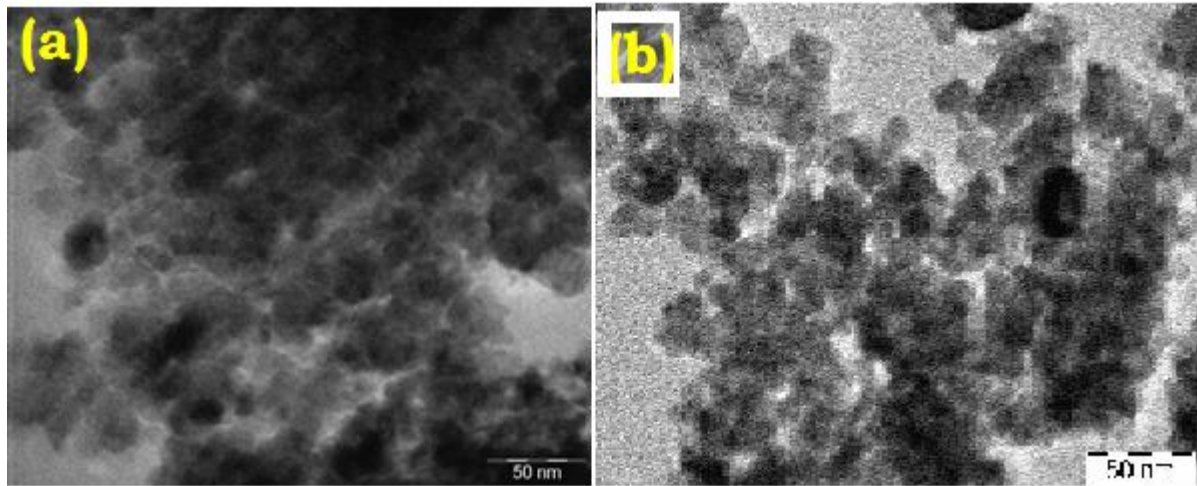


Fig.5.3. TEM images of (a) undoped (b) 0.75 wt% Ba & 0.25wt% Zr co-doped TiO₂ nanomaterial.

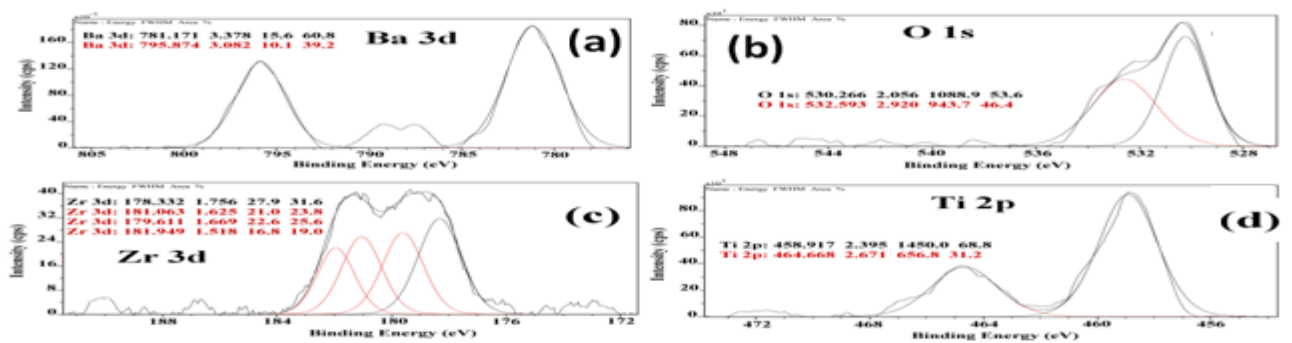


Fig.5.4. (a) XPS survey spectrum of co-doped TiO₂ (b) high resolution spectrum of O 1s (c) Ba 3d (d) O 1s (e) Zr 3d and (f) Ti 2p, respectively.

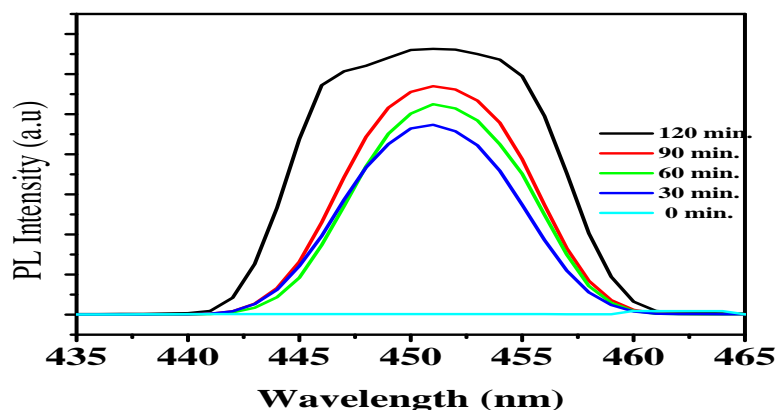
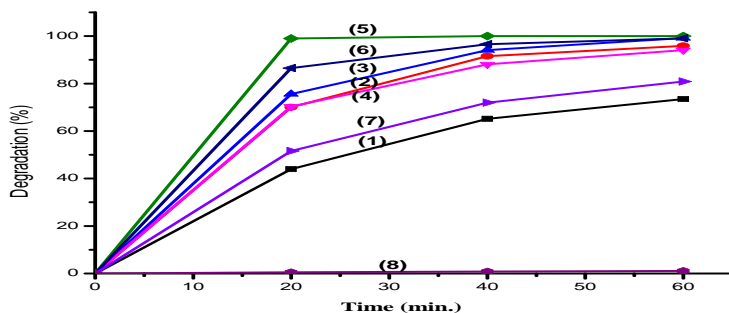


Fig.5.5. PL Photoluminescence spectra of Ba & Zr co-doped showing the release of hydroxyl radicals when irradiated to visible light and the rate of release is very fast in the first few minutes.



- | | |
|--|--|
| 1. 1wt% Ba & 0.25wt% Zr -TiO ₂ | 5. 0.75wt% Ba & 0.25 wt% Zr - TiO ₂ |
| 2. 0.25wt% Ba & 1wt% Zr -TiO ₂ | 6. 0.5wt% Ba & 1wt% Zr - TiO ₂ |
| 3. 0.5wt% Ba & 0.5wt% Zr -TiO ₂ | 7. 1wt% Ba & 0.5wt% Zr - TiO ₂ |
| 4. 0.25wt% Ba & 0.75 Zr wt% Zr- TiO ₂ | 8. Undoped TiO ₂ |

Fig. 6.1. Effect of dopant concentration of co-doped titania on the % degradation of EY. Here the nanomaterial catalyst dosage 0.1g, pH 10 & EY 10 ppm.

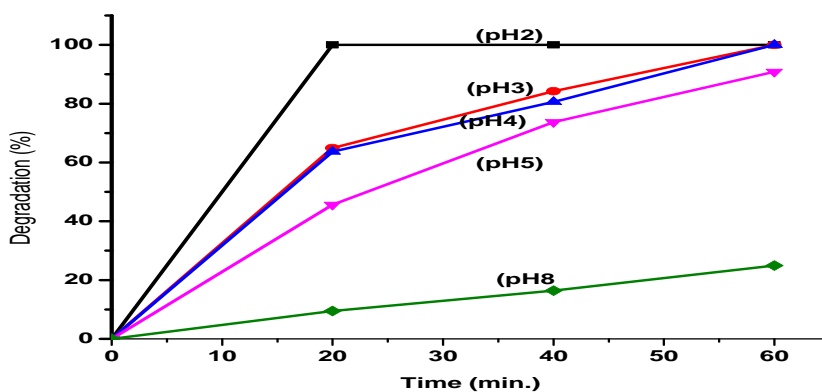


Fig.6.2. The effect of pH on the % degradation of EY by Ba & Zr co-doped TiO₂. Here, catalyst dosage = 0.1g and EY = 10 ppm.

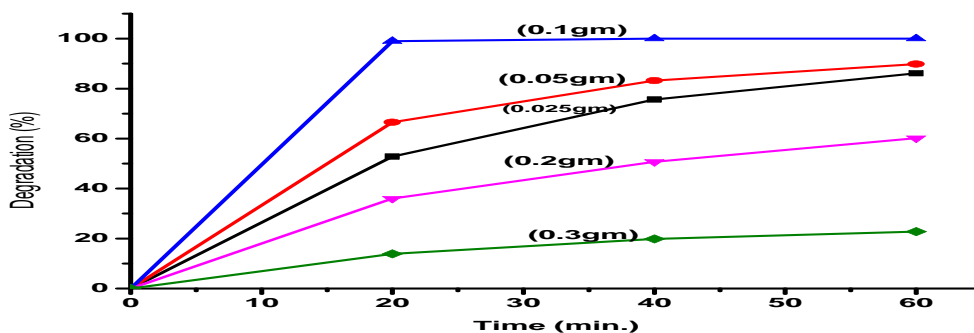


Fig. 6.3. Effect of catalyst dosage on the % degradation of EY by 0.75 wt% Ba & 0.25 wt% Zr co-doped TiO₂ nanomaterial. Here, pH=10 and EY=10 ppm.

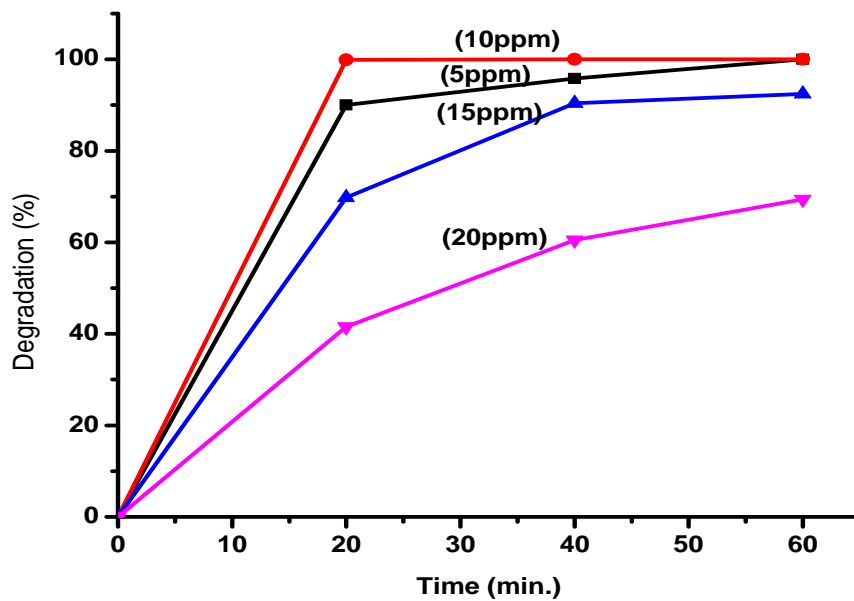


Fig.6.4. The effect of initial concentration of dye on the % degradation of EY. Here pH = 2, catalyst dosage = 0.1g.